

Theoretical framework for microscopic osmotic phenomena

Paul J. Atzberger*

Department of Mathematics, University of California at Santa Barbara, Santa Barbara, California 93106, USA

Peter R. Kramer

Department of Mathematical Sciences, Rensselaer Polytechnic Institute, Troy, New York 12180, USA

(Received 22 December 2006; published 27 June 2007)

The basic ingredient of osmotic pressure is a solvent fluid with a soluble molecular species which is restricted to a chamber by a boundary which is permeable to the solvent fluid but impermeable to the solute molecules. For macroscopic systems at equilibrium, the osmotic pressure is given by the classical van 't Hoff law, which states that the pressure is proportional to the product of the temperature and the difference of the solute concentrations inside and outside the chamber. For microscopic systems the diameter of the chamber may be comparable to the length scale associated with the solute-wall interactions or solute molecular interactions. In each of these cases, the assumptions underlying the classical van 't Hoff law may no longer hold. We develop a general theoretical framework which captures corrections to the classical theory for osmotic pressure under more general relationships between the size of the chamber and the interaction length scales. We also show that notions of osmotic pressure based on the hydrostatic pressure of the fluid and the mechanical pressure on the bounding walls of the chamber must be distinguished for microscopic systems. To demonstrate how the theoretical framework can be applied, numerical results are presented for the osmotic pressure associated with a polymer of N monomers confined in a spherical chamber as the bond strength is varied.

DOI: [10.1103/PhysRevE.75.061125](https://doi.org/10.1103/PhysRevE.75.061125)

PACS number(s): 05.20.-y, 05.70.-a, 05.10.-a

I. INTRODUCTION

Osmotic effects are thought to play an important role in many physical systems associated with biology and technological applications. Examples in technological applications include microscopic devices designed to pump fluids [1–3], actuate forces through swelling [4,5], or deliver drug doses [6–8]. Some macroscopic osmotic mechanisms in biology include the exchange of blood constituents in capillaries with surrounding tissues [9] and the processing of fluids in tissues of layered epithelial cells in the intestines and kidneys [10,11].

At a more microscopic level, individual cells contain a high concentration of charged molecules, in which osmotic effects must be controlled actively to avoid excessive swelling and bursting of cellular structures [12,13]. In fact some of the mechanisms by which neural cells transmit electrical signals through the production and propagation of action potentials may have as their evolutionary origins the pumping mechanisms developed by cells to use counter-ion fluxes to compensate for the harmful effects of osmotic pressure [12,14]. Other examples include the study of the pressures involved in DNA confinement in virus capsids [15], packaging of proteins in small cellular vesicles in cell organelles [16], and even mechanisms of gel swelling in propulsion in micro-organisms such as myxobacteria [3,8,17].

With new experimental techniques, such as optical trapping and molecular tagging, it is now feasible to observe and measure forces and displacements in systems on a length scale of hundreds to tens of nanometers [18,19,21] and the underlying physical processes can begin to be explored

quantitatively at very small length scales in biological and synthetic systems [15,18–20,22,23]. The modeling and analysis of these types of systems motivates using a theoretical framework from statistical mechanics which is general enough to apply to these systems without the usual type of hard-wall and other scale separation assumptions appropriate in classical thermodynamic systems.

In this paper we shall discuss a general microscopic theory for osmotic pressure at equilibrium and draw some contrasts with the classical theory of van 't Hoff [24]. First, in Sec. II, we introduce two statistical quantities to characterize pressure associated with osmotic phenomena: one related to the pressure built up in the fluid and another to the pressure felt by the confining wall of the chamber. We find in Sec. III that while both lead macroscopically to equivalent notions of osmotic pressure, they differ in general for microscopic systems with interaction length scales comparable to the chamber size. Each form of osmotic pressure has theoretical connections to macroscopic thermodynamics: the osmotic wall pressure maintains its statistical mechanical relationship to changes in free energy with respect to volume changes, while the osmotic fluid pressure is directly related to the notion of osmotic pressure in macroscale nonequilibrium thermodynamics. A specific example illustrating the distinctions between the two notions of osmotic pressure and their deviations from the classical van 't Hoff law is presented in Secs. III B and IV, in which noninteracting solutes have a solute-wall interaction potential given by a power law of the distance of the solute to the wall.

We then proceed in Sec. V with an example of solute particles bound by “string”-like forces and confined in a chamber with a hard-walled potential. In this section it is illustrated how the length scale of the solute particle interactions affects the osmotic pressure. After introducing in Sec. VI an alternative expression for the osmotic pressure in

*atzberg@math.ucsb.edu

terms of corrections from the van 't Hoff law, we illustrate in Sec. VII the theoretical formalism through numerical Monte Carlo calculations for the osmotic pressure for a polymer confined within a spherical chamber with various binding strengths (and therefore bond lengths). The theoretical framework presented in this paper is expected to be applicable to model osmotic effects in many microscopic systems at equilibrium and provides a step toward developing a non-equilibrium (or near-equilibrium) theory for microscopic osmotic phenomena.

II. MICROSCOPIC OSMOTIC PRESSURE

We begin by posing two possible means for describing the pressures associated with osmotic phenomena at a microscopic level in a chamber with a confining boundary (wall) permeable to the solvent but not the solute. We are concerned here with developing a microscopic analysis, rather than a macroscale thermodynamic description. In particular, we are interested in a theory based on quantities that could be measured in a microscale experiment or computed from a microscale simulation, using a numerical method, for example, such as the stochastic immersed boundary method [25] or Stokesian dynamics [26].

The first quantity we shall consider is the mechanical pressure exerted by the solute on the wall. The second quantity is the hydrostatic pressure built up in the solvent in the interior of the chamber. While these two notions lead to the same pressure quantities for macroscopic systems, referred to as the osmotic pressure, we shall show that different results are obtained for the pressures when considering microscopic systems.

The osmotic pressure definition based on the wall pressure maintains some classical thermodynamic relationships involving pressure and other statistical mechanical quantities in nonideal systems for which the length scale of the wall and solute interactions are nonzero and finite. On the other hand, the osmotic pressure definition based on the manifested fluid pressure can be shown to be equivalent, in a certain local sense, to the osmotic pressure definition used in the theory of macroscopic nonequilibrium thermodynamics [27,28] to describe the driving force behind solute fluxes across a semipermeable wall or membrane.

Both notions of osmotic pressure therefore have some underlying theoretical justification in both microscopic terms and relation to macroscopic thermodynamics, though we will show through theory and example that they are not equivalent. Both types of pressure, moreover, would appear to have practical relevance for modeling and analysis depending on the application.

When investigating swelling phenomena and the elastic forces of a confining membrane, for example, a notion of pressure involving the average force exerted per unit area on the confining wall may be of particular interest. In contrast, when investigating the role of fluid dynamics in transport and dilution of the concentration of solute, for example, the hydrodynamic pressures which drive the flows may be of more relevance.

In what follows, we generally restrict our attention to the case of N identical and possibly interacting solute particles

confined in the chamber. Furthermore, we shall assume throughout that the potential energy of the particles is of the form

$$\Psi(\mathbf{x}_1, \dots, \mathbf{x}_N) = V(\mathbf{x}_1, \dots, \mathbf{x}_N) + \sum_{k=1}^N \Phi(\mathbf{x}_k). \quad (1)$$

In the notation, $V(\mathbf{x}_1, \dots, \mathbf{x}_N)$ models the energy of the solute-solute interactions and $\Phi(\mathbf{x})$ models the interaction of a solute particle with the chamber wall. The \mathbf{x}_k denote the spatial coordinates for the k th solute particle. Much of the theory can be readily extended to more general potentials.

A. Osmotic wall pressure

The first notion of ‘‘osmotic pressure’’ we consider will be defined in terms of the average forces that solute particles exert on the walls of a confining chamber. We shall assume that the solute-wall interaction potential Φ arises from a uniform areal distribution of particles on the wall which have an isotropic interaction with the solute, given by a potential ϕ . More specifically, we shall assume that for a confined solute particle at interior location \mathbf{x} the interaction force exerted on the differential area $d\mathbf{y}$ of the bounding wall can be expressed as

$$\mathbf{G}(\mathbf{x} - \mathbf{y})d\mathbf{y}, \quad (2)$$

where $\mathbf{G}(\mathbf{r}) = -\nabla_{\mathbf{r}}\phi(|\mathbf{r}|)$ and ϕ is the isotropic interaction potential of the wall particles with the solute particles.

The force acting on a solute particle in the chamber interior which arises from the wall interactions is then given by

$$\mathbf{F}_{\text{wl}}(\mathbf{x}) = \int_{\partial\Omega} -\mathbf{G}(\mathbf{x} - \mathbf{y})d\mathbf{y}, \quad (3)$$

where Ω defines the container volume and $\partial\Omega$ the container boundary, which we often simply call ‘‘a wall.’’ We discuss in the Appendix how the form of the solute-wall interaction (\mathbf{G} or ϕ) can be inferred from an observed or known structure for the wall force \mathbf{F}_{wl} or potential Φ .

To keep focus on the main issues of interest, we will treat the container shape as prescribed and fixed. The results would apply to more general systems with a flexible boundary (such as a membrane-bound vesicle), provided the thermal fluctuations of the bounding surface in equilibrium could be neglected due to their amplitude or time scale. In this case, we would not be predicting self-consistently the shape of the container, but simply taking its (time-averaged) shape in thermal equilibrium as an input to define Ω .

Forces of the form of Eq. (3) can arise in a system in a variety of ways. For example, a solute particle (possibly a macro-ion) in the interior of a chamber could interact with like-charged particles composing the wall surface [29]. In this case, \mathbf{G} would represent the screened Coloumbic force per unit area exerted on the surface as a consequence of the charge density of the wall and solute while \mathbf{F}_{wl} would be the screened Coloumbic force acting on the solute particle when it occupies location \mathbf{x} . In principle, both of these forces could be derived from a common electrostatic potential for the sys-

tem [30]. Another example would be for \mathbf{G} to represent an effective force of interaction between a particle and the wall arising from time-averaged steric interaction forces such as those between a particle and a polymer brush coating the wall [33]. One could even consider within this framework the degrees of freedom of a single monomer of a large, compactly folded polymer as constituting an effective particle confined by the time-averaged effects of the rest of the monomers in the polymer.

To define a pressure for these types of systems we can consider the average forces which act in the normal direction across the wall surface:

$$P_{\text{wl}} = \left\langle \frac{1}{|\partial\Omega|} \int_{\partial\Omega} \sum_{j=1}^n \mathbf{G}(\mathbf{X}^{[j]}(t) - \mathbf{y}) \cdot \hat{\mathbf{n}}_{\mathbf{y}} d\mathbf{y} \right\rangle, \quad (4)$$

where $|\partial\Omega|$ denotes the surface area of bounding wall $\partial\Omega$, $\hat{\mathbf{n}}_{\mathbf{y}}$ denotes the unit outward normal to the surface at \mathbf{y} , and $\langle \cdot \rangle$ denotes a time average over the position of the N solute particles $\{\mathbf{X}^{[j]}(t)\}_{j=1}^N$, which we shall assume is equal to the statistical ensemble average. In the notation, $\mathbf{X}^{[j]}(t)$ denotes the position of solute particle j at time t . We shall refer to this definition of pressure as the ‘‘osmotic wall pressure.’’

We can alternatively express this osmotic wall pressure in terms of the density of the wall-solute interaction potential as

$$\begin{aligned} P_{\text{wl}} &= \left\langle \frac{1}{|\partial\Omega|} \int_{\partial\Omega} \sum_{j=1}^n -\hat{\mathbf{n}}_{\mathbf{y}} \cdot \nabla_{\mathbf{y}} \phi(|\mathbf{X}^{[j]}(t) - \mathbf{y}|) d\mathbf{y} \right\rangle \\ &= \left\langle \frac{1}{|\partial\Omega|} \int_{\partial\Omega} \int_{\Omega} \sum_{j=1}^n -\hat{\mathbf{n}}_{\mathbf{y}} \cdot \nabla_{\mathbf{y}} \phi(|\mathbf{x} - \mathbf{y}|) \right. \\ &\quad \left. \cdot \delta(\mathbf{x} - \mathbf{X}^{[j]}(t)) d\mathbf{x} d\mathbf{y} \right\rangle \\ &= \frac{1}{|\partial\Omega|} \int_{\partial\Omega} \int_{\Omega} -\hat{\mathbf{n}}_{\mathbf{y}} \cdot \nabla_{\mathbf{y}} \phi(|\mathbf{x} - \mathbf{y}|) c(\mathbf{x}) d\mathbf{x} d\mathbf{y}, \quad (5) \end{aligned}$$

where we have introduced the Dirac delta function $\delta(\mathbf{x})$ in order to express the statistical average in terms of the solute concentration [31]:

$$c(\mathbf{x}) := \left\langle \sum_{j=1}^n \delta(\mathbf{x} - \mathbf{X}^{[j]}(t)) \right\rangle. \quad (6)$$

This concentration is proportional to the probability density for any of the particle positions $\mathbf{X}^{[j]}(t)$ to be at location \mathbf{x} when the system is in statistical equilibrium.

B. Osmotic fluid pressure

Another approach to studying osmotic pressure is to consider the solvent fluid and, in particular, how the forces of interaction between the solute and wall are manifested in the hydrostatic pressure. For a Stokesian fluid we have that the local fluid velocity \mathbf{u} satisfies

$$\rho \frac{\partial \mathbf{u}}{\partial t} = -\mu \Delta \mathbf{u} - \nabla p + \mathbf{f} + \mathbf{f}_{\text{th}}, \quad (7)$$

$$\nabla \cdot \mathbf{u} = 0, \quad (8)$$

where ρ is the fluid density, μ is the dynamic viscosity, p is the fluid pressure, \mathbf{f} is the force density exerted by the solute particles, and \mathbf{f}_{th} is the force density associated with thermal fluctuations [25,32,34].

Working with the immersed boundary method approximation [35] for the interaction of a fluid with N identical solute particles, we express

$$\mathbf{f}(\mathbf{x}, t) = \sum_{j=1}^N -\nabla_j \Psi(\Lambda^j) \delta(\mathbf{x} - \mathbf{X}^{[j]}(t)). \quad (9)$$

In the notation, $\mathbf{X}^{[j]}(t)$ denotes the position of solute particle j at time t and ∇_j denotes a gradient with respect to the spatial coordinate of solute particle j . For compactness in the notation we also define convenient expressions involving composite vectors of the particle positions as follows: $\Lambda^j = \Lambda^j(\mathbf{x}, \{\mathbf{X}^{[k]}(t)\}_{k=1, k \neq j}^N) = [\mathbf{X}^{[1]}, \dots, \mathbf{X}^{[j-1]}, \mathbf{x}, \mathbf{X}^{[j+1]}, \dots, \mathbf{X}^{[N]}]^T$ and $\Lambda_j = \Lambda_j(\mathbf{x}, \{\mathbf{x}_k\}_{k=1, k \neq j}^N) = [\mathbf{x}_1, \dots, \mathbf{x}_{j-1}, \mathbf{x}, \mathbf{x}_{j+1}, \dots, \mathbf{x}_N]^T$. The $\delta(\mathbf{x})$ describes the manner in which the force on the solute particles is distributed to the fluid; for small idealized point particles, this would just be the usual Dirac δ function.

More general particle-fluid interaction functions, however, could be used both for modeling and numerical reasons, as in the immersed boundary method [35]. Our end results will generally be posed in a manner which can be appropriate for δ functions with zero or finite width, but for conciseness we will treat the δ functions in derivations as classical Dirac delta functions. Moreover, one could more rigorously describe the fluid-particle interactions in terms of rigid or flexible moving boundaries, but we choose to use the immersed boundary approximation with Dirac δ functions in this initial work since it will convey our central ideas and distinctions with a minimum of technical distraction.

Since no external driving force is applied to the chamber, we have at statistical equilibrium that the average fluid velocity must be $\langle \mathbf{u}(\mathbf{x}) \rangle = 0$ [36], which, along with the fact that the thermal force density \mathbf{f}_{th} has zero mean, implies

$$0 = -\langle \nabla p \rangle + \langle \mathbf{f} \rangle. \quad (10)$$

Expressing the force density \mathbf{f} explicitly in terms of the potentials of the forces acting on the solute particles, we can define an average pressure gradient:

$$\begin{aligned} \nabla \bar{p}(\mathbf{x}) &:= \langle \nabla p(\mathbf{x}) \rangle = \langle \mathbf{f}(\mathbf{x}) \rangle \\ &= \left\langle \sum_{j=1}^N -\nabla_{\mathbf{x}} \Phi(\mathbf{x}) \delta(\mathbf{x} - \mathbf{X}^{[j]}(t)) \right\rangle \\ &\quad + \left\langle \sum_{j=1}^N -\nabla_j V(\Lambda^j) \delta(\mathbf{x} - \mathbf{X}^{[j]}(t)) \right\rangle \\ &= -\nabla_{\mathbf{x}} \Phi(\mathbf{x}) c(\mathbf{x}) + \left\langle \sum_{j=1}^N -\nabla_j V(\Lambda^j) \delta(\mathbf{x} - \mathbf{X}^{[j]}(t)) \right. \\ &\quad \left. \cdot \int_{\Omega^{N-1}} \prod_{k=1, k \neq j}^N (\delta(\mathbf{x}_k - \mathbf{X}^{[k]}(t))) d\mathbf{x}_k \right\rangle \end{aligned}$$

$$\begin{aligned}
 &= -\nabla_{\mathbf{x}}\Phi(\mathbf{x})c(\mathbf{x}) + \sum_{j=1}^N \int_{\Omega^{N-1}} -\nabla_{\mathbf{x}_j}V(\Lambda_j)\rho_N(\Lambda_j) \\
 &\quad \times \prod_{k=1, k \neq j}^N d\mathbf{x}_k. \quad (11)
 \end{aligned}$$

In the notation, $c(\mathbf{x})$ is the local concentration density of the solute as defined in Eq. (6) and

$$\rho_N(\mathbf{x}_1, \mathbf{x}_2, \dots, \mathbf{x}_N) = \left\langle \prod_{j=1}^N \delta(\mathbf{x}_j - \mathbf{X}^{[j]}(t)) \right\rangle \quad (12)$$

is the N -particle correlation function in thermal equilibrium. All terms in the last sum are equal if the particles are truly identical and exchangeable, but we leave the expression as an explicit sum to incorporate systems with bonded interactions. For example, in Sec. VII we consider a confined polymer in which the monomers on the ends have a different bonding structure than monomers in the interior of the polymer chain (ends have only one bond, interior monomers have two).

By integrating the pressure gradient along a path starting from a reference point \mathbf{x}_A outside the domain Ω (where we set the pressure to the reference value of zero), we can thereby define what we will call the ‘‘osmotic fluid pressure’’ $P_{\Pi}(\mathbf{x})$ inside the domain:

$$P_{\Pi}(\mathbf{x}) := \bar{p}(\mathbf{x}) = \int_{\mathbf{x}_A}^{\mathbf{x}} \nabla \bar{p}(\mathbf{x}) \cdot d\mathbf{x}. \quad (13)$$

To compare this notion of pressure with the osmotic wall pressure we shall mostly present the osmotic fluid pressure at the center of the domain (which we shall take to be $\mathbf{x}=0$), but the definition of the osmotic fluid pressure field extends throughout space.

III. STATISTICAL MECHANICAL FORMULAS FOR OSMOTICALLY RELATED PRESSURES

As a starting point for our ensuing analysis, we show how both osmotically related pressures, Eqs. (4) and (13), defined in Sec. II can be represented in terms of the partition function for the solute particles in a soft-walled potential. In Sec. III A, we will verify that for noninteracting particles in the hard-wall limit, we recover the standard van ’t Hoff law for osmotic pressure both on the wall and in the fluid.

We consider first the pressure, Eq. (4), induced by the solute against the chamber wall. In what follows, we will relate the osmotic pressure to changes in the Helmholtz free energy (or equivalently the partition function in the canonical ensemble) under the deformation of the container volume and the formulas will only take familiar statistical mechanical form if we scale the wall-particle interaction force (and energy) density inversely with the local area of the surface. This corresponds to the physical situation in which the number of particles making up the wall, rather than their areal density, remains fixed under deformation. Therefore, we define a one-parameter family of deformations (diffeomorphisms) $\boldsymbol{\eta}_s(\cdot)$ which deform the chamber boundary $\partial\Omega$

$\equiv \partial\Omega(s_0)$ into a new boundary $\partial\Omega(s)$ by extending or contracting the surface at a constant rate along the local outward normal vector $\hat{\mathbf{n}}_{\mathbf{y}}$ at each $\mathbf{y} \in \partial\Omega(s)$. The differential equations describing this family of deformations are

$$\boldsymbol{\eta}_{s_0}(\mathbf{y}) = \mathbf{y}, \quad (14)$$

$$\frac{\partial \boldsymbol{\eta}_s(\mathbf{y})}{\partial s} = \hat{\mathbf{n}}_{\boldsymbol{\eta}_s(\mathbf{y})}. \quad (15)$$

These mappings are generally smooth only over a finite interval of parameters s containing s_0 . Then, taking our ϕ and \mathbf{G} to refer to the potentials and forces associated with the reference chamber surface $\partial\Omega(s_0)$, we define the potential for solute-wall interaction forces in the deformed chamber boundaries through

$$\Phi(\mathbf{x}, s) = \int_{\partial\Omega(s)} \phi(|\mathbf{x} - \mathbf{y}|) \det[\nabla \boldsymbol{\eta}_s^{-1}(\mathbf{y})] d\mathbf{y}, \quad (16)$$

where the Jacobian factor $\det[\nabla \boldsymbol{\eta}_s^{-1}(\mathbf{y})]$ is inversely proportional to the local expansion of area under the deformation. The potential so defined is naturally related to the force defined above in Eq. (3) through $\mathbf{F}(\mathbf{x}) = -\nabla_{\mathbf{x}}\Phi(\mathbf{x}, s_0)$. The total normal force acting outward on the surface of the wall exerted by a solute molecule at location \mathbf{x} is then given by

$$\begin{aligned}
 h(\mathbf{x}) &\equiv \int_{\partial\Omega(s)} -[\hat{\mathbf{n}}_{\mathbf{y}} \cdot \nabla_{\mathbf{y}}\phi(|\mathbf{x} - \mathbf{y}|)] \det[\nabla \boldsymbol{\eta}_s^{-1}(\mathbf{y})] d\mathbf{y} \\
 &= \int_{\partial\Omega(s)} \hat{\mathbf{n}}_{\mathbf{y}} \cdot \nabla_{\mathbf{x}}\phi(|\mathbf{x} - \mathbf{y}|) \det[\nabla \boldsymbol{\eta}_s^{-1}(\mathbf{y})] d\mathbf{y} \\
 &= \int_{\partial\Omega(s_0)} \hat{\mathbf{n}}_{\boldsymbol{\eta}_s(\mathbf{y}')} \cdot \nabla_{\mathbf{x}}\phi(|\mathbf{x} - \boldsymbol{\eta}_s(\mathbf{y}')|) d\mathbf{y}' \\
 &= \int_{\partial\Omega(s_0)} \frac{\partial \boldsymbol{\eta}_s(\mathbf{y}')}{\partial s} \cdot \nabla_{\mathbf{x}}\phi(|\mathbf{x} - \boldsymbol{\eta}_s(\mathbf{y}')|) d\mathbf{y}' \\
 &= -\frac{\partial}{\partial s} \int_{\partial\Omega(s_0)} \phi(|\mathbf{x} - \boldsymbol{\eta}_s(\mathbf{y}')|) d\mathbf{y}' \\
 &= -\frac{\partial}{\partial s} \int_{\partial\Omega(s)} \phi(|\mathbf{x} - \mathbf{y}|) \det[\nabla \boldsymbol{\eta}_s^{-1}(\mathbf{y})] d\mathbf{y} \\
 &= -\frac{\partial \Phi(\mathbf{x}, s)}{\partial s}. \quad (17)
 \end{aligned}$$

The solute concentration $c(\mathbf{x})$ is obtained as a one-particle contraction of the n -particle correlation function:

$$c(\mathbf{x}) = \sum_{j=1}^N \int_{\Omega^{N-1}} \rho_N(\Lambda_j) \prod_{k=1, k \neq j}^N d\mathbf{x}_k, \quad (18)$$

which, in thermal equilibrium, can be expressed in terms of the Boltzmann distribution

$$\rho_N(\mathbf{x}_1, \mathbf{x}_2, \dots, \mathbf{x}_N) = Z(s)^{-1} \exp\left(-\frac{\psi(\mathbf{x}_1, \mathbf{x}_2, \dots, \mathbf{x}_N)}{k_B T}\right), \quad (19)$$

where T is the temperature, k_B is Boltzmann's constant, and the partition function for the solute particles confined by a surface $\partial\Omega(s)$ is given by

$$\begin{aligned} Z(s) &= \int_{\Omega^N} \exp\left(-\frac{\psi(\mathbf{x}_1, \mathbf{x}_2, \dots, \mathbf{x}_N)}{k_B T}\right) \prod_{k=1}^N d\mathbf{x}_k \\ &= \int_{\Omega^N} \exp\left(-\frac{V(\mathbf{x}_1, \mathbf{x}_2, \dots, \mathbf{x}_N)}{k_B T}\right) \\ &\quad \times \exp\left(\frac{-\sum_{j=1}^N \Phi(\mathbf{x}_j, s)}{k_B T}\right) \prod_{k=1}^N d\mathbf{x}_k. \end{aligned} \quad (20)$$

Substituting Eqs. (18) and (17) into Eq. (5), we obtain for the osmotic wall pressure

$$\begin{aligned} P_{\text{wl}} &= \frac{1}{|\partial\Omega|} \int_{\Omega} h(\mathbf{x}) c(\mathbf{x}) d\mathbf{x} \\ &= \frac{1}{|\partial\Omega|} \int_{\Omega} -\frac{\partial\Phi(\mathbf{x}, s)}{\partial s} \sum_{j=1}^N \int_{\Omega^{N-1}} \rho_N(\Lambda_j) \left(\prod_{k=1, k \neq j}^N d\mathbf{x}_k\right) d\mathbf{x} \\ &= \sum_{j=1}^N \frac{1}{|\partial\Omega|} \int_{\Omega^N} -\frac{\partial\Phi(\mathbf{x}_j, s)}{\partial s} \rho_N(\mathbf{x}_1, \mathbf{x}_2, \dots, \mathbf{x}_N) \prod_{k=1}^N d\mathbf{x}_k \\ &= \frac{k_B T}{|\partial\Omega|} \frac{\partial}{\partial s} \ln[Z(s)]|_{s=s_0}, \end{aligned} \quad (21)$$

and in the last expression, we have indicated that the pressure is to be calculated for the initially specified chamber wall $s=s_0$. Our result, Eq. (21), agrees with the thermodynamic definition of pressure as the (functional) derivative of the Helmholtz free energy $-k_B T \ln Z$ with respect to volume V along our one-parameter family of deformations, for which $dV=|\partial\Omega|ds$. We remark that since the bounding walls are assumed to be impermeable to the solute, the confinement energy must diverge at the boundary, $\Phi(\mathbf{x}, s) \rightarrow \infty$ as $\mathbf{x} \rightarrow \partial\Omega(s)$, which has the effect of restricting integration to only the interior of the chamber. The reason that the osmotic wall pressure is only equal to the volume derivative of the free energy along a certain one-parameter family of shape deformations appears to be related to the fact that nonlocal interactions (such as by a soft-wall potential) make the *local* pressure no longer constant within a container, and therefore along the surface, so that different kinds of shape deformations will have different free energy costs per volume of deformation.

Next we develop a statistical mechanical representation for the osmotic fluid pressure, Eq. (13), our second notion of osmotic pressure. We shall again assume that the system at statistical equilibrium has Boltzmann statistics, Eq. (19), from which it follows that the expression for $\nabla\bar{p}(\mathbf{x})$ in Eq. (11) can be simplified as follows:

$$\begin{aligned} \nabla\bar{p}(\mathbf{x}) &= \frac{k_B T}{Z} \nabla_{\mathbf{x}} \sum_{j=1}^N \int_{\Omega^{N-1}} \exp\left(-\frac{\Psi(\Lambda_j)}{k_B T}\right) \prod_{k=1, k \neq j}^N d\mathbf{x}_k \\ &= k_B T \nabla c(\mathbf{x}). \end{aligned} \quad (22)$$

From Eqs. (13) and (22), we obtain

$$P_{\text{fl}}(\mathbf{x}) = k_B T c(\mathbf{x}). \quad (23)$$

This shows that our form of the osmotic fluid pressure connects with macroscopic notions in nonequilibrium thermodynamics [27].

A. Hard-wall limit

We now show how these formulas relate to the van 't Hoff law for osmotic pressure both on the confining wall and in the fluid in the case that the particles are noninteracting and the confining potential has a classical hard-wall potential of the form

$$\Phi(\mathbf{x}, s) = \begin{cases} 0, & \mathbf{x} \in \Omega(s), \\ \infty, & \mathbf{x} \notin \Omega(s). \end{cases} \quad (24)$$

Substitution of this ‘‘hard-walled’’ confining potential into Eq. (20), we have that $Z(s)$ is just the N th power of volume $V(s)$ of the chamber $\Omega(s)$. By Eq. (21), the osmotic wall pressure is then

$$P_{\text{wl}} = k_B T c_0, \quad (25)$$

where $c_0=N/V(s_0)$ is the concentration, recovering the well-known van 't Hoff law equation [24]. Similarly, from Eq. (23), we have

$$P_{\text{fl}}(\mathbf{x}) = \frac{Nk_B T [V(s_0)]^{N-1}}{Z(s_0)} = \frac{Nk_B T}{V(s_0)} = k_B T c_0, \quad (26)$$

and again find that the classical van 't Hoff law is recovered in the fluid pressure.

We remark that the key to obtaining the classical van 't Hoff law in both cases was to consider the hard-walled limit of the confining potentials which arises naturally when the length scale of particle-wall interactions are very small relative to the diameter of the confining chamber. In this regime a theory similar to our approach was developed in [4], in which a careful analysis is made of the balance of mechanical forces arising from the solute interactions with the walls, again under the assumption that the chamber diameter is much larger than the length scale of the particle interaction forces. While this assumption typically holds for macroscopic systems, when the chamber size becomes sufficiently small, the results of this limit are no longer strictly valid and corrections are required to the classical theory reflecting some of the microscopic features of the system.

B. Steric interactions with the chamber walls of non-negligible length scale

For microscopic systems, the length scale on which the solute particles interact with the wall may be non-negligible relative to the diameter of the chamber. For example, if a

rigid spherical particle of radius ℓ is confined in a spherical chamber having radius R , the steric interactions would confine the particle center to have only configurations with $|\mathbf{x}| < R - \ell$. We shall now illustrate how this affects the osmotic pressure when ℓ is comparable in size to R .

More precisely, in the case of a spherical chamber of radius R the confinement potential is of the general form

$$\Phi(\mathbf{x}, R) = \int_{\partial\Omega(R)} \phi(|\mathbf{y} - \mathbf{x}|) \frac{R_0^2}{R^2} d\mathbf{y}, \quad (27)$$

where $\phi(\rho)$ denotes the solute-wall potential for a given reference sphere of radius R_0 and $\det[\nabla \boldsymbol{\eta}_s^{-1}(\mathbf{y})] = R_0^2/R^2$. Now for $R_* = R - \ell < R$ we have

$$\phi(\rho) = \begin{cases} 0, & \rho \geq \ell, \\ \infty, & \rho < \ell, \end{cases} \quad (28)$$

where $\rho = |\mathbf{y} - \mathbf{x}|$. By radial symmetry this gives for $r = |\mathbf{x}|$ the solute confinement potential

$$\Phi(r, R) = \begin{cases} 0, & r \leq R - \ell, \\ \infty, & r > R - \ell. \end{cases} \quad (29)$$

The partition function and its derivative are obtained explicitly as

$$Z(R) = \frac{4\pi}{3} (R - \ell)^3, \quad (30)$$

$$\frac{\partial Z(R)}{\partial R} = 4\pi (R - \ell)^2. \quad (31)$$

From Eq. (13), the osmotic fluid pressure is given by

$$P_{fl}(\mathbf{0}) = \frac{k_B T}{\frac{4\pi}{3} (R - \ell)^3}. \quad (32)$$

From Eq. (21), the osmotic-wall pressure is given by

$$P_{wl} = \frac{k_B T}{Z} = \frac{k_B T}{\frac{4\pi}{3} (R - \ell)^3} \left(1 - \frac{\ell}{R}\right)^2, \quad (33)$$

where $\ell < R$.

The difference in these two notions of pressure in this case can be interpreted geometrically. In particular, the confinement forces restrict the solute particles within a spherical region of radius $R_* = R - \ell$. This has the effect of generating within the confinement region the same local confinement forces as a hard-walled potential with a wall occupying the spherical shell of radius $R_* = R - \ell$ and yields the same osmotic-fluid pressure as in the hard-walled case. However, the particle-wall interactions, which generate the confinement forces, occur from a wall occupying the spherical shell of radius R , as opposed to a spherical shell of radius R_* as would occur in the strictly ‘‘hard-wall’’ case. From the principle of equal and opposite forces, the particle-wall interactions now exert forces in the normal direction over a wall with greater surface area than in the short-range hard-wall case, thus reducing the osmotic wall pressure by the geomet-

ric factor $(1 - \ell/R)^2 = (R_*/R)^2$, which is the ratio between the surface areas.

While this example is rather special, it illustrates clearly one mechanism by which differences with the classical theory of osmotic pressure can arise. This also illustrates how notions of osmotic pressure in terms of the wall pressure and fluid pressure can differ markedly when the length scales of the particle-wall interactions become comparable to the diameter of the chamber. We next demonstrate how osmotic pressures behave for smooth potentials having long-range particle-wall interactions.

IV. OSMOTIC PRESSURE FOR NONINTERACTING SOLUTE PARTICLES CONFINED BY A SOFT-WALLED POTENTIAL

We now examine the behavior of the osmotic pressure for a system of noninteracting solute particles which interact with the chamber wall through a smooth long-range potential. For simplicity, we will consider the osmotic pressure exerted by a single solute particle; the case of N noninteracting solute particles of course simply multiplies the pressures by a factor of N . We shall consider here the class of repulsive potentials for a spherical chamber of radius R_0 of the form

$$\phi(\rho) = C\rho^{-\alpha}, \quad (34)$$

which, under volume dilations to new radii R , induce effective wall potentials

$$\Phi(r, R) = \frac{2\pi C R_0^2 (1-r)^{2-\alpha} - (1+r)^{2-\alpha}}{R^\alpha (\alpha-2)r}. \quad (35)$$

We consider only $\alpha > 2$ to ensure that $\lim_{r \rightarrow R} \Phi(r, R) = \infty$.

The partition function and its derivative can be expressed as

$$Z(R) = 4\pi R^3 \int_0^1 \exp\left(-\frac{(1-r)^{2-\alpha} - (1+r)^{2-\alpha}}{(\alpha-2)\lambda r}\right) r^2 dr \quad (36)$$

and

$$\begin{aligned} \frac{\partial Z}{\partial R} &= \frac{3Z(R)}{R} + \frac{4\pi R^2}{\lambda} \left(\frac{\alpha}{\alpha-2}\right) \\ &\times \int_0^1 \left(\frac{(1-r)^{2-\alpha} - (1+r)^{2-\alpha}}{r}\right) \\ &\times \exp\left(-\frac{(1-r)^{2-\alpha} - (1+r)^{2-\alpha}}{(\alpha-2)\lambda r}\right) r^2 dr, \end{aligned} \quad (37)$$

where $\lambda = k_B T R^\alpha / 2\pi C R_0^2$ can be regarded as a reduced temperature. These expressions were obtained by using Eqs. (16) and (20) with $R = s$ and making the change of variable $r = Rr'$. This gives the osmotic fluid pressure

$$P_{\text{fl}}(\mathbf{0}) = \frac{k_B T}{\frac{4\pi}{3}R^3} Q_1(\lambda, \alpha) \quad (38)$$

$$P_{\text{wl}} = \frac{k_B T}{\frac{4\pi}{3}R^3} Q_2(\lambda, \alpha), \quad (39)$$

and the osmotic wall pressure

where

$$Q_1(\lambda, \alpha) = \exp\left(-\frac{2}{\lambda}\right) \left[3 \int_0^1 \exp\left(-\frac{(1-r)^{2-\alpha} - (1+r)^{2-\alpha}}{(\alpha-2)\lambda r}\right) r^2 dr \right]^{-1} \quad (40)$$

and

$$Q_2(\lambda, \alpha) = 1 + \left(\frac{1}{3\lambda}\right) \left(\frac{\alpha}{\alpha-2}\right) \frac{\int_0^1 \left(\frac{(1-r)^{2-\alpha} - (1+r)^{2-\alpha}}{r}\right) \exp\left(-\frac{(1-r)^{2-\alpha} - (1+r)^{2-\alpha}}{(\alpha-2)\lambda r}\right) r^2 dr}{\int_0^1 \exp\left(-\frac{(1-r)^{2-\alpha} - (1+r)^{2-\alpha}}{(\alpha-2)\lambda r}\right) r^2 dr}. \quad (41)$$

For this system with the power-law potential, we can express Q_1 compactly as

$$Q_1 = \frac{\frac{4}{3}\pi R^3}{Z(R)} \exp\left(-\frac{2}{\lambda}\right) \quad (42)$$

and Q_2 as

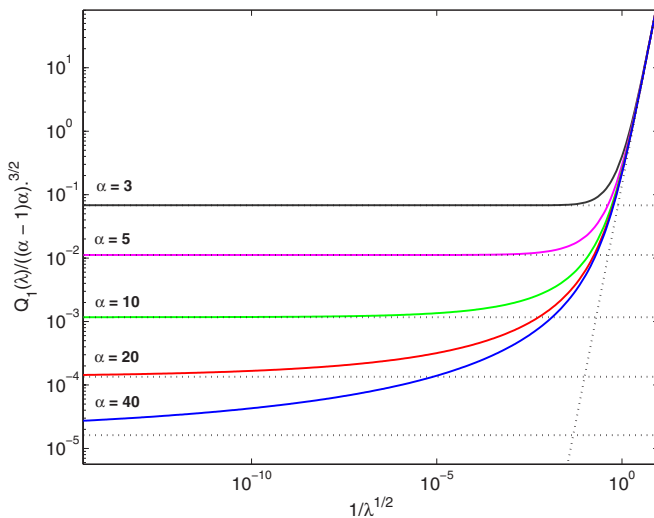


FIG. 1. (Color online) Q_1 Correction factor for a soft-walled potential. For $\lambda \rightarrow \infty$ we have $1/\lambda^{1/2} \rightarrow 0$ and $Q_1 \rightarrow 1$. This corresponds to the plotted horizontal lines. For $\lambda \rightarrow 0$ we have $1/\lambda^{1/2} \rightarrow \infty$ and $Q_1/[(\alpha-1)\alpha]^{3/2} \sim (\frac{9\sqrt{3}\pi}{4}\lambda^{3/2})^{-1}$. This corresponds to the plotted diagonal line on the right.

$$Q_2(\lambda, \alpha) = 1 + \frac{\alpha}{3} \left\langle \frac{(1-r)^{2-\alpha} - (1+r)^{2-\alpha}}{(\alpha-2)\lambda r} \right\rangle = 1 + \frac{\alpha \langle \Phi \rangle}{3k_B T}. \quad (43)$$

The last expression shows that Q_2 is 1 plus a term proportional to the ensemble average of the energy of the system over all configurations of the confined particle with respect to the Boltzmann distribution.

We observe first of all that the soft-walled nature of the potential produces corrections to the van 't Hoff law for the osmotic pressure of the chamber in both the osmotic wall pressure and fluid pressure. To compare these correction factors with each other, we first examine their asymptotic behaviors in the limits $\lambda \rightarrow 0$ and $\lambda \rightarrow \infty$. Note that the term λ represents the ratio of the energy scale of the thermal fluctuations relative to that of the confining potential, and therefore these limits correspond to low-temperature and high-temperature limits, respectively. As $\lambda \rightarrow \infty$ we have $Q_1, Q_2 \rightarrow 1$, which recovers the hard-walled limit. On the other hand, for small λ , $Q_1 \sim [\frac{9\sqrt{3}\pi}{4}(\frac{\lambda}{(\alpha-1)\alpha})^{3/2}]^{-1}$ and $Q_2 \sim 2\alpha/3\lambda$, showing a behavior similar to a system at low temperature in which the structure of the long-range particle-wall interactions plays a significant role. We note that the correction factors for the osmotic fluid pressure and osmotic wall pressure diverge at different rates with respect to λ as $\lambda \rightarrow 0$, indicating that the osmotic fluid and wall pressures will deviate significantly both from each other and from the van 't Hoff law for soft-walled confining potentials with energy scales large compared to the temperature. On the other hand, plots of the behavior of the correction factors as a function of $1/\lambda^{1/2}$ (see Figs. 1 and 2) show qualitatively similar behavior, in that the ratio of the osmotic pressures to the values given by the van 't Hoff law increases monotonically from 1 as $1/\lambda^{1/2}$ increases and diverges as $\lambda \rightarrow 0$.

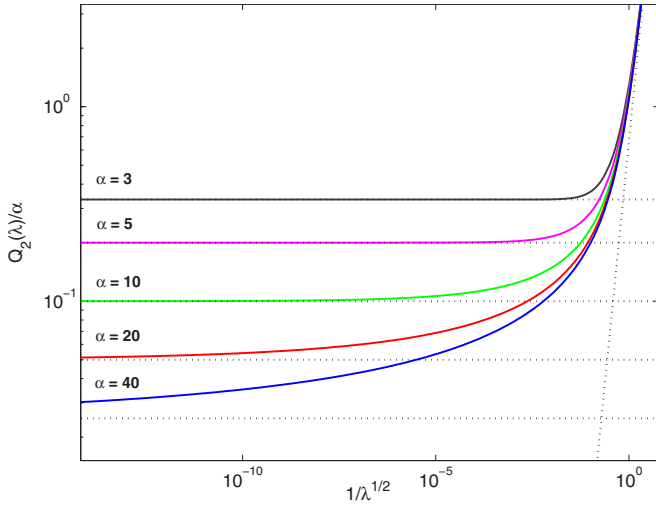


FIG. 2. (Color online) Q_2 Correction factor for a soft-walled potential. For $\lambda \rightarrow \infty$ we have $1/\lambda^{1/2} \rightarrow 0$ and $Q_2 \rightarrow 1$. This corresponds to the plotted horizontal lines. For $\lambda \rightarrow 0$ we have $1/\lambda^{1/2} \rightarrow \infty$ and $Q_2/\alpha \sim 2/3\lambda$. This corresponds to the plotted diagonal line on the right.

V. OSMOTIC PRESSURE OF SOLUTE DIMERS CONNECTED BY “STRINGS” AND CONFINED BY A HARD-WALLED POTENTIAL

We shall now discuss how the length scale of interaction between the solute particles can affect the osmotic pressures when this length scale is comparable to the chamber size. To illustrate through analytical formulas the basic mechanism by which this occurs, we shall consider the rather special case of two solute particles which are connected by a “string” and confined by a “hard-walled” spherical potential. More precisely, the potential energy of the system is given by

$$\Psi(\mathbf{x}_1, \mathbf{x}_2, R) = \Phi(\mathbf{x}_1, R) + \Phi(\mathbf{x}_2, R) + V(\mathbf{x}_1, \mathbf{x}_2), \quad (44)$$

where Φ is the hard-wall potential given in Eq. (24). The potential V models the interaction between the two solute particles, located at \mathbf{x}_1 and \mathbf{x}_2 , and is given by

$$V(\mathbf{x}_1, \mathbf{x}_2) = \begin{cases} 0, & \text{if } |\mathbf{x}_2 - \mathbf{x}_1| < \ell, \\ \infty, & \text{otherwise.} \end{cases} \quad (45)$$

This potential can be given the physical interpretation of no coupling between the two particles until they attempt to separate past a distance ℓ , at which point an infinitely strong restoring force constrains the particles to be a distance less than or equal ℓ . This form of coupling is analogous to connecting the two particles by an inelastic “piece of string” of length ℓ . The osmotic pressure for M noninteracting strings would of course just multiply the 1-string pressures we calculate by M .

Using this form of the potentials we have

$$\Psi(\mathbf{x}_1, \mathbf{x}_2, R) = \begin{cases} 0, & (\mathbf{x}_1, \mathbf{x}_2) \in \Gamma(R, \ell), \\ \infty, & (\mathbf{x}_1, \mathbf{x}_2) \in \Gamma^c(R, \ell), \end{cases} \quad (46)$$

where

$$\Gamma(R, \ell) = \{ (\mathbf{x}_1, \mathbf{x}_2) \mid |\mathbf{x}_1| < R, |\mathbf{x}_2| < R, |\mathbf{x}_2 - \mathbf{x}_1| < \ell \}, \quad (47)$$

with Γ the admissible region in $\mathbb{R}^3 \times \mathbb{R}^3$ in which both of the solute particles are a distance no more than ℓ apart and contained within the spherical chamber of radius R . In this case, the partition function can be expressed in terms of a few quantities having a straightforward geometric interpretation and computed exactly. In particular, the partition function

$$Z(R) = \int_{\Omega^2} \exp\left(-\frac{\Psi(\mathbf{x}_1, \mathbf{x}_2, R)}{k_B T}\right) d\mathbf{x}_1 d\mathbf{x}_2 \quad (48)$$

is the volume of the region $\Gamma(R, \ell) \subset \mathbb{R}^6$.

To compute this volume, we shall find it convenient to split the configuration space into two parts: $\Gamma^{(1)}(R, \ell) = \{|\mathbf{x}_1| < R - \ell\}$ and $\Gamma^{(2)}(R, \ell) = \{R - \ell < |\mathbf{x}_1| < R\}$, where it is to be understood that $\Gamma^{(1)}, \Gamma^{(2)} \subset \Gamma$. In the first region, for each \mathbf{x}_1 the second particle \mathbf{x}_2 is free to assume values within the entire sphere of radius ℓ about \mathbf{x}_1 having volume $\frac{4\pi}{3}\ell^3$. In the second region, for each \mathbf{x}_1 the second particle \mathbf{x}_2 must lie within the intersection of the sphere of radius ℓ centered at \mathbf{x}_1 and the sphere of radius R centered at $\mathbf{0}$. The volume of the region so defined will be denoted by $W_\star(|\mathbf{x}_1|)$. Using this decomposition, the partition function can be expressed as

$$\begin{aligned} Z(R) &= \int_{\Gamma^{(1)}} \frac{4\pi}{3} \ell^3 d\mathbf{x}_1 + \int_{\Gamma^{(2)}} W_\star(|\mathbf{x}_1|) d\mathbf{x}_1 \\ &= \left(\frac{4\pi}{3} \ell^3\right) \left(\frac{4\pi}{3} (R - \ell)^3\right) + 4\pi \int_{R-\ell}^R W_\star(r) r^2 dr, \end{aligned} \quad (49)$$

where the volume W_\star can be expressed as

$$W_\star(r) = C(R, h_1(r)) + \frac{4\pi}{3} \ell^3 - C(\ell, h_2(r)), \quad (50)$$

with C denoting the volume of a spherical cap of height h for a sphere of radius r (see Fig. 3):

$$C(r, h) = \frac{1}{3} \pi h^2 (3r - h). \quad (51)$$

Here $h_1(r) = R - u_0(r)$ is the height of the spherical cap c_3 and $h_2(r) = r + \ell - u_0(r)$ is the height of the spherical cap c_2 , where $u_0(r) = (r^2 - \ell^2 + R^2)/2r$ is the radius corresponding to the plane which contains the intersection of the two spheres (Fig. 3).

From this the exact solution for the partition function and its derivative can be computed to obtain

$$Z(R, \ell) = \frac{16}{9} \pi^2 R^3 \ell^3 - \pi^2 R^2 \ell^4 + \frac{1}{18} \pi^2 \ell^6 \quad (52)$$

and

$$\frac{\partial Z}{\partial R}(R, \ell) = \frac{16}{3} \pi^2 \ell^3 R^2 - 2\pi^2 R \ell^4. \quad (53)$$

The osmotic pressures are then given for $\ell < R$ by

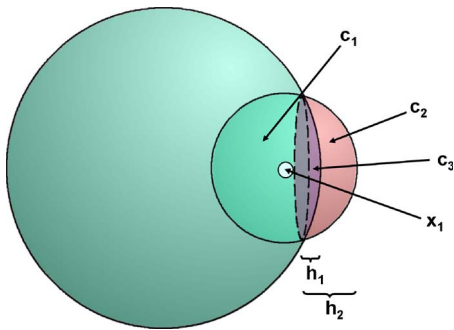


FIG. 3. (Color online) Geometry of the intersection of two spheres. The surfaces of any two spheres intersect in a circle carried in a common plane (dashed circle). We shall refer to this as the “plane of intersection” and further assume that the center of the smaller sphere lies within the volume of the larger sphere. For any such plane we may define three volumes by “slicing” the small and large spheres along this plane. We let c_1 denote the volume the sliced part of the larger sphere lying to the left of the “plane of intersection.” We let c_2 denote the volume associated with the sliced part of the small sphere lying to the right of the “plane of intersection.” We let c_3 denote the volume associated with the sliced part of the larger sphere lying to the right of the “plane of intersection.” To characterize the numerical values of the volume of these regions we define h_1 to be height of the spherical cap c_3 and h_2 the height of the spherical cap c_2 .

$$P_{\text{fl}}(\mathbf{0}) = \frac{2k_B T}{4\pi R^3} \left(\frac{1}{1 - \frac{9}{16} \left(\frac{\ell}{R}\right) + \frac{1}{32} \left(\frac{\ell}{R}\right)^3} \right), \quad (54)$$

$$P_{\text{wl}} = \frac{k_B T}{4\pi R^3} \left(\frac{1 - \frac{3}{8} \left(\frac{\ell}{R}\right)}{1 - \frac{9}{16} \left(\frac{\ell}{R}\right) + \frac{1}{32} \left(\frac{\ell}{R}\right)^3} \right). \quad (55)$$

This gives the correction to the classical theory when the interactions of the solute particles becomes non-negligible relative to the diameter of the chamber. For $\ell > 2R$, the particle interaction becomes trivial and both osmotic wall and fluid pressure assume the van 't Hoff [24] law value of $2k_B T / \frac{4}{3} \pi R^3$.

The above expressions verify that in the limit $\ell \rightarrow 0$, the osmotic wall pressure converges to the classical van 't Hoff pressure $k_B T / \frac{4}{3} \pi R^3$ of a single confined particle. This is to be expected as the two-particle string should coalesce into a single entity in the tight-binding limit. A similar transition between van 't Hoff law behavior for the osmotic wall pressure exerted by dimers in the weak-binding and tight-binding limits was shown for springlike dimers in numerical simulations with the stochastic immersed boundary method in [25].

The osmotic fluid pressure, by contrast, approaches the value $2k_B T / \frac{4}{3} \pi R^3$ as $\ell \rightarrow 0$, which corresponds to the van 't Hoff law for two particles in a sphere, even though the two particles are tightly bound. This provides another example for how the pressure built up in the fluid near the center need

not be directly linked in magnitude to the pressure exerted by the solute particles on the chamber wall.

VI. CORRECTIONS TO THE VAN 'T HOFF LAW FOR INTERACTING PARTICLES IN SPHERICAL CHAMBERS WITH SOFT-WALLED POTENTIALS

We shall now consider the more general case of N interacting solute particles confined in a spherical chamber of radius R with a soft-walled potential of the form

$$\Psi(\mathbf{x}_1, \dots, \mathbf{x}_N, R) = V(\mathbf{x}_1, \dots, \mathbf{x}_N) + \sum_{k=1}^N \Phi(\mathbf{x}_k, R), \quad (56)$$

where $V(\mathbf{x}_1, \dots, \mathbf{x}_N)$ models the interactions between the particles and $\Phi(\mathbf{x}_k, R)$ confines the k th solute particle to the interior of the chamber, with $\Phi \rightarrow \infty$ as $|\mathbf{x}_k| \rightarrow R$.

From Eqs. (20) and (21), the osmotic pressure can be expressed as

$$P_{\text{wl}} = \frac{Nk_B T}{\frac{4}{3} \pi R^3} + \frac{1}{4\pi R^2} \left(\sum_{k=1}^N \langle -\nabla_{\mathbf{x}_k} V(\mathbf{x}_1, \mathbf{x}_2, \dots, \mathbf{x}_N) \cdot \mathbf{x}_k \rangle \right) + \frac{1}{4\pi R^2} \left(\sum_{k=1}^N \left\langle -\nabla_{\mathbf{x}_k} \Phi(\mathbf{x}_k, R) \cdot \mathbf{x}_k - \frac{\partial \Phi(\mathbf{x}_k, R)}{\partial R} \right\rangle \right), \quad (57)$$

where $\mathbf{x} = (\mathbf{x}_1, \dots, \mathbf{x}_N)$ and $\langle \cdot \rangle$ denotes the ensemble average over the particle configurations weighted by the Boltzmann factor $\exp(-\Psi/k_B T)$. This was derived by making the change of variable $\mathbf{x} = R\mathbf{x}'$ in Z and differentiating in $R = s$.

This expression can be used to characterize the corrections to the classical theory and the relative contributions of the microscopic effects of the system. The first term is the classical pressure one would expect from the van 't Hoff law. The second term arises from the particle-particle interactions, and the third term is from the particle-wall interactions. It is important to note that while we have described the source of each distinct term, the terms in fact are coupled by the ensemble average which depends on the combination of these effects.

The second correction term has an intuitive interpretation as follows. Since the contribution to the pressure is of the form $-\nabla V \cdot \mathbf{x}$, we have that when the particle interaction force acting on any particle is toward the chamber center, the force acting on the bounding wall will be relieved and a negative contribution will be made to the pressure. This suggests one mechanism by which polymerization reduces osmotic pressure relative to free monomers. For a polymer in a typical configuration, most of the monomers will, for entropic reasons, be outside a boundary layer of the wall. As a consequence, any individual monomer that makes an excursion toward the wall would on average experience a pulling force toward the chamber center. From the second correction term this will reduce the osmotic pressure relative to free monomers. This perspective also provides another way of interpreting the wall pressure results for the string model from Sec. V.

The third term gives the corrections that arise from long-range interactions of the solute particles with the boundary wall. In the hard-walled limit this term approaches zero.

We observe that the correction terms to the van 't Hoff law in Eq. (57), other than the partial derivative with respect to chamber radius R , take the form of the virial from classical mechanics. Virial expansions of the pressure can be found in several statistical mechanical textbooks [28] to describe departures of a dilute gas or solution from an ideal noninteracting particle limit. These results are, however, generally developed within the context of a large macroscopic chamber, whereas our focus is on systems for which interaction length scales become comparable to those of the chamber.

VII. OSMOTIC PRESSURE OF CONFINED POLYMERS

To illustrate how this theory can be applied in practice, we now present some numerical results for a model of a polymer chain of N monomers confined in a spherical chamber with a hard-walled confining potential. The monomers of the polymer will have a coupling given by the harmonic bonding energy:

$$V(\mathbf{x}_1, \dots, \mathbf{x}_N) = \sum_{j=2}^N \frac{K}{2} |\mathbf{x}_j - \mathbf{x}_{j-1}|^2. \quad (58)$$

The osmotic pressure of the system can be computed from Eq. (57), which in this case reduces to

$$P_{wl} = \frac{Nk_B T}{\frac{4}{3}\pi R^3} + \frac{1}{4\pi R^2} \sum_{k=1}^n \langle -\nabla_{\mathbf{x}_k} V \cdot \mathbf{x}_k \rangle. \quad (59)$$

We will focus on how the osmotic pressure behaves as the bonding strength K is varied so that the length scale $L = \sqrt{6k_B T/K}$ of bond fluctuations varies between lengths small and large relative to the chamber size. For very small $K \ll 6k_B T/R^2$ the fluctuations in the bond length are expected to be very large and the N monomers to behave independently. For very large $K \gg 6k_B T/R^2$ the fluctuations in the bond length are expected to be very small and the N monomers to behave similarly to a single particle. Thus in the extreme cases the classical osmotic pressures are expected, corresponding to an N -particle or single-particle system.

To obtain the osmotic wall pressure for intermediate values of K , the correction factors were estimated numerically using the Monte Carlo method with Metropolis sampling [37]; see Fig. 4. We find that as the bond stiffness $K \rightarrow 0$, the osmotic wall pressure approaches the classical van 't Hoff osmotic pressure for N free monomers. As $K \rightarrow \infty$ we find that the osmotic wall pressure approaches the classical van 't Hoff osmotic pressure for a single particle. The numerical results show how the theoretical framework can be used to capture the regime relevant to microscopic chambers, such as a polymer confined in a vesicle, in which the bond length is comparable to the chamber size. As can be seen from Fig. 4, the transition between the extremes in the bonding strength is gradual and occurs smoothly in K . A similar numerical study

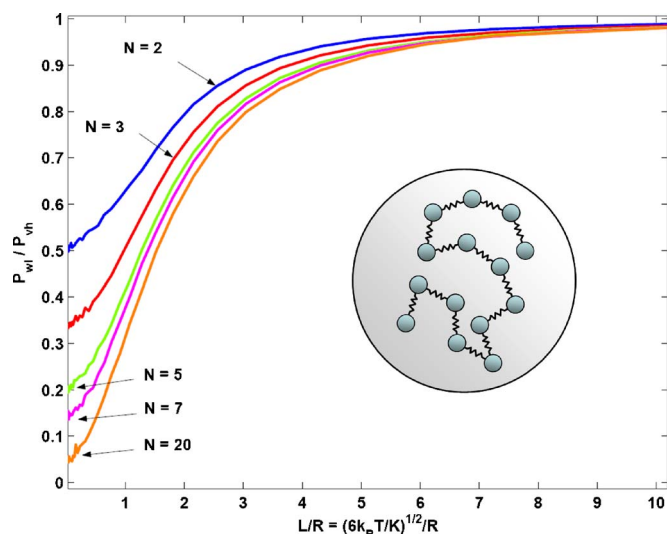


FIG. 4. (Color online) Osmotic pressure of a confined polymer and correction factor for a linear polymer confined in a spherical chamber. The classical van 't Hoff law for N free monomers is $P_{vh} = Nk_B T / \frac{4}{3}\pi R^3$. For stretching an individual bond between monomers, we let $L = (6k_B T/K)^{1/2}$ denote the length at which the bond energy becomes $3k_B T$.

for the osmotic pressure of polymers was conducted within the stochastic immersed boundary method in [25].

VIII. CONCLUSION

We have shown that the osmotic pressure deviates markedly from classical macroscopic theories when the length scale of the system becomes sufficiently small so that the chamber diameter is comparable in size to the length scale of the interactions of the solute particles. In particular, we have explored two ways in which this can occur, through either interactions among the solute molecules or interactions of the solute molecules with the wall. While the classical formulas are not directly applicable in this regime, we have shown that a theoretical framework for the equilibrium osmotic pressures can still be developed provided additional microscopic features of the system are taken into account. We considered how the osmotic pressure is manifested in terms of forces exerted on the confining wall and in terms of the hydrostatic pressure of the fluid in the interior of the chamber. We showed through several examples how these notions of osmotic pressure can differ for microscopic chambers. In particular, we showed how the osmotic wall pressure of a two particle string and an N -particle polymer interpolate between the van 't Hoff laws associated with the extremes of strong and weak bonding, which give effectively a single particulate entity or many individual particulate entities.

While the osmotic fluid pressure is related in a simple local manner to the osmotic pressure defined in nonequilibrium thermodynamics [27,28], it behaves a bit less intuitively. This was demonstrated for the two-particle string, where the tight-binding limit produced an osmotic fluid pressure corresponding to two particulate entities. This is in contrast to the osmotic wall pressure which reflected a single

confined entity. The distinction appears to be related to the local nature of the osmotic fluid pressure, which can vary throughout the chamber and in particular differ between the wall region and center of the chamber. Fluid pressure is only expected to be constant in mechanical equilibrium when the solute-wall forces in the system are local, but here we have been considering interactions between particles and walls on length scales comparable to the chamber size. An important consequence is that the fluid pressure need not be constant throughout the chamber interior and the pressure felt by the wall need not be equal to the buildup in fluid pressure in the chamber center.

The theoretical framework presented here should be readily applicable to the study of equilibrium osmotic phenomena in many microscopic physical systems arising in biology and technological applications. While only equilibrium systems were considered here, it may be possible to use many of the central ideas of this theory to ultimately formulate a nonequilibrium (or near-equilibrium) theory for microscopic osmotic phenomena.

ACKNOWLEDGMENTS

The first author was supported by NSF VIGRE Postdoctoral Research Grant No. DMS-9983646 and NSF Mathematical Biology Grant No. DMS-0635535. The second author was partially supported by NSF CAREER Grant No. DMS-0449717. The authors would like to thank Charles Peskin, George Oster, Philip Pincus, and Frank Brown for helpful suggestions.

APPENDIX: OBTAINING THE PARTICLE-WALL INTERACTION FORCE AND POTENTIAL FROM THE CONFINEMENT FORCE AND POTENTIAL (INVERSION FORMULAS)

From Eq. (4) we see that in order to obtain explicit expressions for the osmotic pressure it is useful to have an expression for $\mathbf{G}(|\mathbf{x}-\mathbf{y}|)$. In modeling systems, we may readily have only the confining force $\mathbf{F}_{\text{wl}}(\mathbf{x})$ while the detailed particle-wall interaction forces must somehow be inferred. For radial symmetric potentials of the form $\mathbf{F}_{\text{wl}}(\mathbf{x}) = F(|\mathbf{x}|)\frac{\mathbf{x}}{|\mathbf{x}|}$ and $\mathbf{G}(\mathbf{r}) = G(|\mathbf{r}|)\frac{\mathbf{r}}{|\mathbf{r}|}$, this requires solving the following inverse problem for G given F :

$$-F(|\mathbf{x}|)\frac{\mathbf{x}}{|\mathbf{x}|} = \int_{\partial\Omega} G(|\mathbf{y}-\mathbf{x}|)\frac{\mathbf{x}-\mathbf{y}}{|\mathbf{x}-\mathbf{y}|} d\mathbf{y}. \quad (\text{A1})$$

By dotting both sides with $\frac{\mathbf{x}}{|\mathbf{x}|}$, this becomes the scalar problem

$$-F(|\mathbf{x}|) = \int_{\partial\Omega} G(|\mathbf{y}-\mathbf{x}|)\frac{\mathbf{x}-\mathbf{y}}{|\mathbf{x}-\mathbf{y}|} \cdot \frac{\mathbf{x}}{|\mathbf{x}|} d\mathbf{y}. \quad (\text{A2})$$

In spherical coordinates, the integral transform can be expressed as

$$-F(r) = \frac{-\pi R}{r^2} \int_{R-r}^{R+r} G(\rho)(r^2 - R^2 + \rho^2) d\rho, \quad (\text{A3})$$

where $\rho = |\mathbf{x}-\mathbf{y}|$ and $r = |\mathbf{x}|$.

To ensure a unique solution to the inverse problem we shall make the assumption that the particle-wall interactions occur only over a distance less than the radius R from the chamber wall—that is, $g(\rho) = 0$ for $\rho \geq R$. Under this assumption the transform can be inverted exactly with the solution formula

$$g(\rho) = \left(\frac{1}{2\pi R \rho^2} \right) \left((R+\rho)F(R-\rho) + \rho(R-\rho)F'(R-\rho) + \int_0^{R-\rho} F(s) ds \right), \quad (\text{A4})$$

from which $G(\rho)$ is readily obtained.

Alternatively, for a given wall potential $\Phi(\mathbf{x}, R)$ the inverse problem is to determine a $\phi(\rho)$ so that for all \mathbf{x}

$$\Phi(\mathbf{x}, R) = \int_{|\mathbf{y}|=R} \phi(|\mathbf{x}-\mathbf{y}|) d\mathbf{y}. \quad (\text{A5})$$

In the case that the potential Φ is radially symmetric in $r = |\mathbf{x}|$, a change of variable allows for the integral to be expressed as

$$\Phi(r, R) = \frac{2\pi R}{r} \int_{R-r}^{R+r} \phi(\rho) \rho d\rho. \quad (\text{A6})$$

A unique solution can be found for this problem under the assumption that $\phi(\rho) = 0$ for $\rho \geq R$. By differentiating both sides in r and substituting $\rho = R - r$, the following inversion formula is obtained:

$$\phi(\rho) = \frac{1}{2\pi R \rho} \left(\Phi(R-\rho, R) + (R-\rho) \frac{\partial \Phi}{\partial r}(R-\rho, R) \right). \quad (\text{A7})$$

- [1] P. A. Atzberger and C. S. Peskin (unpublished).
 [2] M. Z. Bazant and T. M. Squires, Phys. Rev. Lett. **92**, 066101 (2004).
 [3] J. Nardi, R. Bruinsma, and E. Sackmann, Phys. Rev. Lett. **82**, 5168 (1999).
 [4] D. C. Guell and H. Brenner, Ind. Eng. Chem. Res. **35**, 3004

- (1996).
 [5] Y. C. Su, L. Lin, and A. P. Pisano, J. Microelectromech. Syst. **11**, 736 (2002).
 [6] F. Theeuwes and S. I. Yum, Ann. Biomed. Eng. **4**, 343 (1976).
 [7] R. K. Verma, D. M. Krishna, and D. Garg, J. Controlled Release **79**, 7 (2002).

- [8] C. W. Wolgemutha, A. Mogilner, and G. Oster, *Eur. Biophys. J.* **33**, 146158 (2004).
- [9] H. T. Hammel, *FASEB J.* **13**, 213 (1999).
- [10] P. P. Duquette, P. Bissonnette, and J. Y. Lapointe, *Proc. Natl. Acad. Sci. U.S.A.* **98**, 3796 (2001).
- [11] K. R. Spring, *News Physiol. Sci.* **4**, 92 (1999).
- [12] F. C. Hoppensteadt and C. S. Peskin, *Modeling and Simulation in Medicine and the Life Sciences* (Springer-Verlag, New York, 2002).
- [13] G. Oster and C. S. Peskin, in *Swelling Mechanics: From Clays to Living Cells and Tissues*, edited by T. Karalis (Springer-Verlag, Berlin, 1992), pp. 731–742.
- [14] P. Douzou, *Proc. Natl. Acad. Sci. U.S.A.* **91**, 1657 (1994).
- [15] A. Evilevitch, L. Lavelle, C. M. Knobler, E. Raspaud and W. M. Gelbart, *Proc. Natl. Acad. Sci. U.S.A.* **100**, 92929295 (2003).
- [16] B. Alberts, A. Johnson, J. Lewis, M. Raff, K. Roberts, and P. Walker, *Molecular Biology of the Cell* (Garland, London, 2002).
- [17] C. W. Wolgemutha and G. Oster, *J. Mol. Microbiol. Biotechnol.* **7**, 7277 (2004).
- [18] K. C. Neuman and S. M. Block, *Rev. Sci. Instrum.* **75**, 2787 (2004).
- [19] A. Ponti, P. Vallo-ton, W. Salmon, C. Waterman-Storer, and G. Danuser, *Biophys. J.* **84**, 3336 (2003).
- [20] A. Einstein, *Investigations on the Theory of the Brownian Movement* (Dover, New York, 1926).
- [21] J. Lippincott-Schwartz and G. H. Patterson, *Science* **300**, 4 (2003).
- [22] V. G. Levich, *Physico-Chemical Hydrodynamics* (Prentice-Hall, Englewood Cliffs, NJ, 1962).
- [23] R. Lipowsky, in *Statistical Mechanics of Biocomplexity* (Springer-Verlag, Berlin, 1999), pp. 1–32.
- [24] J. H. van 't Hoff, *Z. Phys. Chem., Stoechiom. Verwandtschaftsl.* **1**, 481 (1887).
- [25] P. J. Atzberger, P. R. Kramer, and C. S. Peskin, *J. Comput. Phys.* (to be published).
- [26] J. F. Brady and G. Bossis, *Annu. Rev. Fluid Mech.* **20**, 111 (1988).
- [27] A. Katchalsky and P. F. Curran, *Nonequilibrium Thermodynamics in Biophysics* (Harvard University Press, Cambridge, MA, 1965), Chap. 10.
- [28] L. E. Reichl, *A Modern Course in Statistical Physics*, 2nd ed. (Wiley, New York, 1998).
- [29] A. Y. Grosberg, T. T. Nguyen, and B. I. Shklovskii, *Rev. Mod. Phys.* **74**, 329 (2002).
- [30] V. M. Prabhu, *Curr. Opin. Colloid Interface Sci.* **10**, 2 (2005).
- [31] R. Kubo, M. Toda, and N. Hashitsume, *Statistical Physics. II*, 2nd ed. (Springer-Verlag, Berlin, 1991), Sec. IV.
- [32] L. D. Landau and E. M. Lifshitz, *Statistical Physics*, Vol. 9 of *Course of Theoretical Physics* (Pergamon Press, Oxford, 1980), Chap. IX.
- [33] P. Auroy, Y. Mir, and L. Auvray, *Phys. Rev. Lett.* **69**, 93 (1992).
- [34] L. D. Landau and E. M. Lifshitz, *Fluid Mechanics*, Vol. 6 of *Course of Theoretical Physics* (Butterworth-Heinemann, Oxford, 1987), Chap. II.
- [35] C. S. Peskin, *Acta Numerica* **11**, 1 (2002).
- [36] S. R. de Groot, *Thermodynamics of Irreversible Processes* (North-Holland, Amsterdam, 1951), Chap. 45.
- [37] D. P. Landau and K. Binder, *A Guide to Monte Carlo Simulations in Statistical Physics* (Cambridge University Press, New York, 2000).